Title

Lumbar spinal cord microglia exhibited increased activation in aging dogs compared with young adult dogs.

Journal

GeroScience, 42(1)

Authors

Garcia, Virginia
Snyder, John
Jones, Maria
et al.

Publication Date

2020-02-01

DOI

10.1007/s11357-019-00133-8

Peer reviewed

GeroScience (2020) 42:169–182
https://doi.org/10.1007/s11357-019-00133-8

ORIGINAL ARTICLE

Lumbar spinal cord microglia exhibited increased activation in aging dogs compared with young adult dogs

Christine M. Toedebusch · Virginia B. Garcia · John C. Snyder · Maria R. Jones · David J Schulz · Gayle C. Johnson · Eric Villalón · Joan R. Coates · Michael L. Garcia

Received: 15 August 2019 / Accepted: 30 October 2019 / Published online: 11 December 2019

Abstract Altered microglia function contributes to loss of CNS homeostasis during aging in the brain. Few studies have evaluated age-related alterations in spinal cord microglia. We previously demonstrated that lumbar spinal cord microglial expression of inducible nitric oxide synthase (iNOS) was equivalent between aging, neurologically normal dogs and dogs with canine degenerative myelopathy (Toedebusch et al. 2018, Mol Cell Neurosci. 88, 148-157). This unexpected finding suggested that microglia in aging spinal cord have a pro-inflammatory polarization. In this study, we reexamined our microglial results (Toedebusch et al. 2018, Mol Cell Neurosci. 88, 148-157) within the context of aging rather than disease by comparing microglia in aging versus young adult dogs. For both aging and young adult dogs, the density of microglia was significantly higher closest to the motor neuron cell body. However, there was no difference in densities between aging versus young adult dogs at all distances except for the furthest distance analyzed. The number of motor neurons with polarized microglia was higher in aging dogs; yet, the density per motor neuron of arginase-1-expressing microglia was reduced in aging dogs compared with young adult dogs. Finally, aging dogs had increased steady-state mRNA levels for genes consistent with activated microglia compared with young adult dogs. However, altered mRNA levels were limited to the lumbar spinal cord. These data suggested that aging dog spinal cord microglia exhibit regional immunophenotypic differences, which may render lumbar motor neurons more susceptible to age-related pathological insults.

Keywords Canine · Aging · Microglia · Neurodegeneration

Electronic supplementary material The online version of this article (https://doi.org/10.1007/s11357-019-00133-8) contains supplementary material, which is available to authorized users.

C. M. Toedebusch
Department of Surgical and Radiological Sciences, School of Veterinary Medicine, University of California – Davis, 2112 Tupper Hall, Davis, CA 95616, USA

M. R. Jones · E. Villalón · M. L. Garcia (✉)
Division of Biological Sciences University of Missouri, 1200 University Avenue, 209A LeFevre Hall, Columbia, MO 65211, USA
e-mail: garciaml@missouri.edu

V. B. Garcia · D. J. Schulz
Division of Biological Sciences University of Missouri, 612 Hitt St, 117 Tucker Hall, Columbia, MO 65211, USA

G. C. Johnson · J. R. Coates
Department of Veterinary Medicine and Surgery University of Missouri, 800 E Campus Dr., Columbia, MO 65211, USA

J. C. Snyder
Department of Statistics, University of Missouri, Columbia, MO 65211, USA

Introduction

Comprising only 5–20% of the adult brain in most species, microglia are essential for central nervous system (CNS) homeostasis (Graeber 2010; Svahn et al. 2014; Tremblay et al. 2010; Tremblay et al. 2011). Microglia influence homeostasis through a broad range of effector functions determined by environmental stimuli (Nimmerjahn et al. 2005; Tremblay et al. 2011), including inflammatory responses, activity-dependent synaptic patterning (Schafer et al. 2012; Tremblay et al. 2011), and direct modulation of astrocytic and neuronal activity (Tremblay et al. 2011). While most of the microglial population is renewed throughout life, turnover is slow. Recent estimates suggest that individual microglial cells in the aged human brain can be decades old (Reu et al. 2017). It has been well established that microglia play a central role in age-related neurodegenerative disease pathogenesis (Beers et al. 2006; Boillée et al. 2006; Isobe et al. 2014; Krabbe et al. 2013; Varnum and Ikezu 2012). Accordingly, it is critical to examine the effects of aging on microglial effector function, as it is likely that there are age-related alterations in environmental stimuli contributing to microglia-mediated pathology during aging.

It has been suggested that microglia have altered phenotypes in aged versus young brains, which could represent altered microglial effector function during aging (Conde and Streit 2006). Murine microglia lose homogeneous tissue distribution with aging, suggestive of a diminished capacity for chemotaxis and subsequent immune surveillance of the CNS (Hefendehl et al. 2014). Additionally, aged brain microglia are more immunologically primed for antigen presentation, as evidenced by increased expression of MHC II and complement receptor 3 (CD11b) in brain microglia of several aged species (Frank et al. 2006; Godbout et al. 2005; Sheffield and Berman 1998). Consistent with microglial priming, aged murine microglia have enhanced pro-inflammatory polarization, with reduced anti-inflammatory polarization (Lee et al. 2013). Furthermore, immune challenge of aged microglia results in regionally specific, prolonged, and exaggerated neuroinflammatory responses (Godbout et al. 2005; Xie et al. 2003). Taken together, these findings suggest that aged microglia have a diminished capacity to maintain CNS homeostasis through decreased surveillance and polarization toward a pro-inflammatory phenotype.

In recent years, the companion dog has emerged as a valuable, comprehensive model for human aging and age-related human disease (Urfer et al. 2017a; Urfer et al. 2017b). While there is a paucity of literature regarding microglia in the aged dog, evidence suggests that spinal cord microglia are altered with aging similar to murine models (Ahn et al. 2011; Chung et al. 2010). Increased cell body size and shorter processes has been reported in aged dog spinal cord microglia compared with young adult dog microglia (Chung et al. 2010). Increased ionized calcium-binding adapter molecule 1 (Iba-1) protein has been observed in aged dog spinal cord homogenate, which may be the result of increased total spinal cord microglia with aging (Ahn et al. 2011). Furthermore, increases of pro-inflammatory (interleukin-1 beta (IL-1β) and interferon gamma (IFN-γ); Chung et al. 2010) and oxidative molecules (4-hydroxy-2E-nonenal (4-HNE) and superoxide dismutase-1 (SOD1); Ahn et al. 2011) have been observed in aged dog spinal cord homogenate. We have recently demonstrated that the number of pro-inflammatory microglia near motor neurons, as assessed by expression of inducible nitric oxide synthase (iNOS), was indistinguishable between DM-affected and aging, neurologically normal dogs (Toedebusch et al. 2018). These data are contrary to rodent models of ALS, which demonstrate an upregulation of both neuroprotective and neurotoxic molecules throughout disease progression (Chiu et al. 2013; Liao et al. 2012; Nikodemova et al. 2014). Given that aging is a major risk factor in the development of degenerative myelopathy (DM) (Awano et al. 2009; Coates and Wininger 2010), we hypothesized that aging dog spinal cord microglia are polarized toward a pro-inflammatory phenotype, which may contribute to the onset of canine DM.

In this study, we analyzed microglial responses within the context of aging by comparing young adult (1 year of age), neurologically normal dogs to aging (≥ 8 years of age), neurologically normal dogs using well-characterized markers of microglial phenotype (iNOS and arginase-1) (Lewis et al. 2014). Furthermore, to gain insight into regional specificity of age-related changes, we compared mRNA levels of well-characterized markers for microglial activation status (Liao et al. 2012) (Chiu et al. 2013) from cervical and lumbar spinal cord segments.

Materials and methods

Case selection and sample collection

Aging dog data used in this study has been previously published (Toedebusch et al. 2018). Aging companion dogs (8 years of age or older) were presented to the University of Missouri between July 2012 and March 2016 for euthanasia and donation for research purposes. All pet owners signed an informed consent form (approved by the University of Missouri Animal Care and Use Committee, protocol #8339). Young adult dogs (1 year of age) used in this study were research dogs housed at the University of Missouri in compliance with the National Institutes of Health Guide for the Care and Use of Laboratory Animals and approved by the University of Missouri Animal Care and Use Committee (protocol #8339). All dogs had normal neurological examinations and normal histopathology of the caudal thoracic spinal cord. Information regarding age, breed, sex, and weight are provided in Supplementary Table 1.

Dogs were humanely euthanized and tissue samples were collected. The fourth lumbar (L4) and eighth cervical (C8) spinal segments were isolated; the dura mater was removed, and the segment was hemisected. The spinal cord was divided into halves. The left half was prepared for immunofluorescence studies, and the right half was flash frozen for gene expression assays. Briefly, the left half was immersion fixed in 10% neutral buffered formalin, cryoprotected with 30% sucrose solution, and stored at − 80 °C until sectioning, at which time 30-μm transverse serial sections were made through the segment with a Leica CM1900 cryostat at − 20 °C. Three consecutive sections were pooled in each well and stored in a cryoprotective solution at − 20 °C prior to immunostaining.

Immunofluorescence

Three sections/dog were randomly selected to represent cranial, middle, and caudal L4 sections for immunostaining. Tissue was washed three times for 5 min with Tris-buffered saline with 0.5% Triton X-100 (TBST) (Sigma) at room temperature (RT) and blocked for 1 h at RT on a shaker (10% normal goat serum, 1% bovine serum albumin in TBST). For microglia identification, rabbit polyclonal antibody anti-ionized calcium-binding adaptor molecule (Iba-1) (Wako Pure Chemical Industries, Ltd., Chuo-Ku, Osaka, Japan; 1:1000) was used. To provide microglia phenotype information, co-application of mouse monoclonal antibody anti-arginase-1 (eBioscience, San Diego, CA, USA; 1:400) or mouse monoclonal anti-inducible nitric oxide synthase (iNOS) (EMD Millipore Corporation, Temecula, CA, USA; 1:400) was used. Sections were incubated overnight at 4 °C in primary antibody. The sections were washed three times for 5 min in TBST at RT and incubated with IgG (heavy and light) anti-mouse or anti-rabbit secondary antibodies that were conjugated with either Alexa Fluor 488 or 555 (Molecular Probes, Invitrogen, Carlsbad, CA, USA; 1:1000) diluted in fresh blocking buffer at RT for 1 h. Tissue was then washed three times for 5 min at RT. Tissue was mounted with

Table 1 Primer sets used for real-time PRC reactions. Accession numbers are provided for each gene of interest. Primer sets were generated using PRIMER3 software. All primer sets were validated as described in the "Methods" section

Gene name	Accession #	Forward primer (5′ to 3′)	Reverse primer (5′ to 3′)
ApoE	XM_005616460	TCTGGTATCCCTGAGTCCTAC	AACCTTCATCTTCCAGCCG
Arg1	XM_532053	GAGGAGGGGTGGAAAAAGG	TAGGGACATCAACAAAGGGC
C1QA	XM_535367	TTCAGTGGCTTCCTCATCTTC	GAGCGGACCATAGAAACCAG
IGF1	NM_001313855	GAGGCTAGAGATGTACTGTGC	AGTTCTTGTTTCCTGCACTCC
IL1RA	NM_001003096	TGTGTCCATTCCGTGCTTC	GGGCTCTCATACATCCTTCTG
IL6	NM_001003301	GAGGGCTGTTCGGATAATGTAG	TGACTGGAGAAAGGAATGCC
iNOS	NM_001313848	CGGGACTTCTGTGATGTTCAG	TGGAGTACAGCGACATTGATC
TNF-alpha	NM_001003244	CAACTGGAGAAGGGTGATCG	TGATTCCAAAGTACACCTGCC
TREM2	XM_005627313	AATCATAAAGCCAGACCCCAG	TCGTCTTTCCCTTGAGTTGC
GAPDH	NM_001003142	TGCACCACCAACTGCTTAGC	GGCATGGACTGTGGTCATGAG

Vectashield with 4′,5-diamidino-2phenylindole (DAPI) (Vector Labs, Burlingame, CA, USA).

Microglia quantification and phenotype determination

Alpha motor neurons were identified by autofluorescence, location within the ventral horn, and their relatively large size. Individual motor neurons were centered in the imaging field, and images were collected in a *z*-plane at 1-μm sections throughout the depth of each motor neuron at 63X. All alpha motor neurons identified in each section were imaged separately. Post-imaging, three concentric circles were drawn around the neuronal soma via ImageJ software. Each circle had an increasing radius of 6 μm, the average microglial cell body diameter (Toedebusch et al. 2018).

Microglial quantification and phenotyping were conducted in a double-blinded manner. Each blinded counter recorded the number of microglial cells within each ring as determined by Iba-1 immunoreactivity (IR). To ensure cells were not counted twice, the nucleus must have been visible to count the cell. To phenotype microglial cells, we evaluated protein expression of reciprocal enzymes involved in arginine metabolism within microglial cell bodies, arginase-1, and inducible nitric oxide synthase (iNOS) (Morris Jr. 2004). Arginase-1 expression has been correlated with neuroprotective phenotypes, whereas iNOS expression has been correlated with neurotoxic phenotypes (Colton 2009). Microglia cells that were double-labeled (Iba-1 and arginase-1 or iNOS) were counted. Counts were normalized to the volume of tissue sampled in cubic meters.

Quantitative polymerase chain reaction

For spinal cord tissue samples, total RNA was isolated using Trizol as per manufacturer's protocol (Invitrogen). cDNA was generated from 500 ng total RNA primed with a mixture of oligo-dT and random hexamers that was reverse transcribed using qScript cDNA SuperMix (QuantaBio). The final volume of the reverse transcription reaction was 20 μL, and following heat inactivation of the enzyme, samples were diluted in ultrapure water to a final volume of 100 μL.

We designed or modified, and independently validated primer sets for use in absolute quantitation of copy number for 9 distinct genes of interest (see Table 1). These primer sets amplified genes that are associated with pro-inflammatory (*INOS*, *IL-6*, *TNF-α*), anti-inflammatory (*ARG-1*, *IGF1*, *ILIRA*), and phagocytic (*APOE*, *C1QA*, *TREM2*) microglia. Primer sets were designed using Primer3 software (Untergasser et al. 2012). These primer sets are listed in Table 1. Validation for each set of primers was performed using a 4× cDNA serial dilution series from young dog spinal cord as a template. We evaluated the efficiency and fit of the curves generated. We rejected any primer set that did not produce an efficiency of at least 0.9 and an R^2 value of 0.95 from the cDNA dilution series. Only experimental quantification cycle (Cq) values that fell within the boundaries of the validated curves were used for analysis.

qPCR reactions consisted of primer pairs at a final concentration of 2.5 μM, 5 μL cDNA template, and SSoAdvanced Universal SYBR Green Supermix (BioRad) per manufacturer's protocol. Reactions were carried out on a CFXConnect (BioRad) machine with a three-step cycle of 95 °C, 15 s; 60 °C, 20 s; and 72 °C, 20 s, followed by a melt curve ramp from 65 to 95 °C. Data were acquired during the 72 °C step, and every 0.5 °C of the melt curve. All reactions were run as 10 μL triplicates, and the average Cq used as the data point for a given sample. Care was taken at each step to minimize assay variability: samples were processed in parallel, the same batch of reverse transcriptase was used for all samples, and PCR runs were designed to maximize the number of samples run in each batch.

Statistics

Microglial quantification

The primary tool used for the statistical analysis of volume normalized total cell counts was a generalized linear mixed effects model using group (young adult, aging), ring (1, 2, 3), and their potential interaction as fixed effects. As there may have been variability associated within individuals as well as the particular spinal sections that were examined, the ID of the dog, as well as the section, was considered as random effects. Furthermore, the sections were different between the dogs, so we considered the section effect to be nested within the effect of the dogs. Because the normalized total cell count was right skewed, strictly positive value, the gamma distribution was used to model the response variable, with plots empirically demonstrating this distribution to be an excellent fit. An example of the

histogram of the normalized total cell counts and corresponding gamma fit produced by this approach was previously published (Toedebusch et al. 2018).

To evaluate variable significance, a full model containing all fixed effects was compared with one without the variable under consideration. If a likelihood ratio test determined these two fit models to be statistically different, it was the case that the variable provides significant contribution to the model and should be retained. When the variable was not significant, it was removed, and the model without that term became the new model under consideration. Once a final model was reached, pairwise comparisons with a Tukey adjustment were used to compare across groups within a ring, and between rings within a group to examine the effect of these variables.

Microglia phenotype determination

In this analysis, we examined if a microglial cell was arginase-1 positive or iNOS positive separately. Thus, a large proportion of phenotype observations have "0" counts. As the gamma distribution used previously requires the response to be strictly positive and there was an excess of "0" counts for phenotype determination, this analysis was conducted in a two-step approach. In step 1, a logistic regression was used to examine the probability of having a positive count for a particular phenotype compared with not observing any cells of that phenotype. This allowed us to determine if there were any defining characteristics in the rings or groups that yield "0" or nonzero counts. In step 2, we considered only those observations that had positive counts and used a generalized linear model to examine how the counts varied between the groups and rings. As before, a full model containing all fixed effects was compared with one without the variable under consideration to evaluate variable significance. Again, when a final model was determined, we examined plots and pairwise comparisons for comparing the rings and groups.

To compare the proportion of motor neurons with closely associated activated microglia between aging and young adult dogs, a two sample Z test of proportions was performed (Table 2). To compare the proportion of anti- and pro-inflammatory microglia within the activated microglia population of the aging and young adult groups, a one-sample proportion test was used.

qPCR

Fold difference in expression between young adult and aging animals was calculated and plotted using the $\Delta\Delta$Cq method with glyceraldehyde 3-phosphate dehydrogenase (GAPDH) as the control gene for normalization and relative expression (Livak 1997). There were no significant differences in GAPDH expression between any of the groups measured. All data were expressed as fold expression change relative to young adult animals. For statistical analyses, data were confirmed to be normally distributed and passed an equal variance test, and then mean ΔCq compared between young adult and aging groups for a given gene via unpaired t tests.

Results

Aging dog microglia exhibited an activated morphology

Consistent with previous reports in the dog (Chung et al. 2010) and other species (Boche et al. 2013; Chung et al. 2010; Crain et al. 2013), we observed morphologic

Table 2 Quantification of the number of motor neurons with activated microglia expressing iNOS (pro-inflammatory) or Arg-1 (anti-inflammatory) proteins. Aging dogs had more motor neurons with closely associated activated microglia compared with young adult dogs (74% vs. 18%; $p < 0.0001$). Of the activated microglia observed, young adult dogs had a higher proportion of anti-inflammatory microglia (76% vs. 24%; $p = 0.0009$), while aging dogs had an equivalent distribution between anti- and pro-inflammatory microglia (52% vs. 48%; $p = 0.36$)

	Young adult dogs		Aging dogs	
# MN examined	223		227	
Total # (%) MN with activated microglia	41 (18%)		168 (74%)	
Distribution between pro- and anti-inflammatory microglia	iNOS	Arg-1	iNOS	Arg-1
	10 (24%)	31 (76%)	81 (48%)	87 (52%)

differences between microglia from young adult and aging dogs. A ramified morphology, exhibited by many fine processes, was observed in young adult dogs (Fig. 1a). On the contrary, microglia from aging dogs commonly exhibited decreased process ramification consistent with activation (Fig. 1b) (Conde and Streit 2006).

Young adult and aging dogs had equivalent numbers of microglia in close approximation to the motor neuron, but aging dogs had increased microglia outside the ring system

To examine the microglia cell number in close proximity to motor neurons of the lumbar spinal cord, we used a modified Sholl's method (Sholl 1953) to apply a ring system around the cell body of L4 alpha motor neurons (Fig. 2a). Microglial number was increased closest (ring 1) to the motor neuron cell body for both young adult and aging dogs (Fig. 2b). For young adult dogs, the increase was significant for ring 1 compared with ring 3 ($p < 0.0001$) and outside the ring ($p < 0.0001$). In aging dogs, the increase was statistically significant for ring 1 versus all other rings ($p < 0.0001$ all comparisons). Microglial number was not significantly different between young adult dogs versus aging within the rings (ring 1, $p = 0.5567$; ring 2, $p = 0.4763$; ring 3, $p = 0.5554$). However, aging dogs had increased microglia outside the ring system compared with young adult dogs ($p = 0.0025$).

Arginase-1-expressing microglia were increased in close approximation to motor neurons in young adult dogs

To begin phenotyping microglial cells, we evaluated protein expression of reciprocal enzymes involved in arginine metabolism within microglial cell bodies, arginase-1, and inducible nitric oxide synthase (iNOS) (Morris Jr. 2004). While arginase-1 was detected in both young adult and aging dog microglia (Fig. 3a, b), iNOS was rarely detected in adult dog microglia (Fig. 3c). A subset of aging dog microglia had positive immunoreactivity (IR) for iNOS (Fig. 3d).

Using a generalized linear model, we examined the probability of identifying arginase-1- or iNOS-expressing microglia in close approximation to motor neurons and outside the ring system. Compared with young adult dogs, there was a greater probability of identifying arginase-1-expressing microglia within (Fig. 4a; $p < 0.001$) and outside (Fig. 4c; $p < 0.001$) the ring system in aging dogs. Similarly, there was a greater probability of identifying iNOS-expressing microglia in aging dogs within ($p < 0.001$) and outside the ring system ($p < 0.001$) compared with young adult dogs. Moreover, in both young adult and aging dogs, there was a greater probability of identifying microglial cells expressing arginase-1 and iNOS outside the ring system versus within the ring system (young adult dogs, $p = 0.0011$; aging dogs, $p < 0.001$).

Given the probability of identifying a double-labeled microglia cell around a motor neuron was greater in aging dogs compared with young adult dogs, we quantified the total number of motor neurons with closely associated double-labeled microglia (Table 2). Of the 227 motor neurons evaluated in aging dogs, 168 (74%) of them had closely associated arginase-1- ($n = 87$) or iNOS-expressing ($n = 81$) microglia (Table 2). Conversely, few young adult dog motor neurons had closely associated double-labeled microglia (41/223 (18%)). Taken together, aging dogs had more motor neurons with closely associated activated microglia compared with young

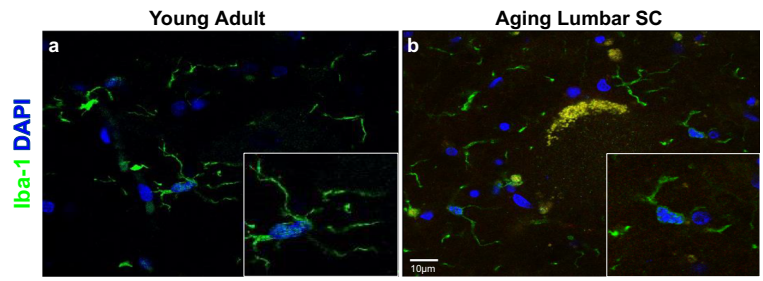

Fig. 1 Microglia in aging lumbar spinal cords exhibited morphology consistent with activation. Representative images of lumbar spinal cord microglia (Iba-1; green). **a** Microglia from young adult dogs tended to have long, branching processes. **b** A subset of microglia from aging dogs exhibited decreased ramification of their processes, which was consistent with activation

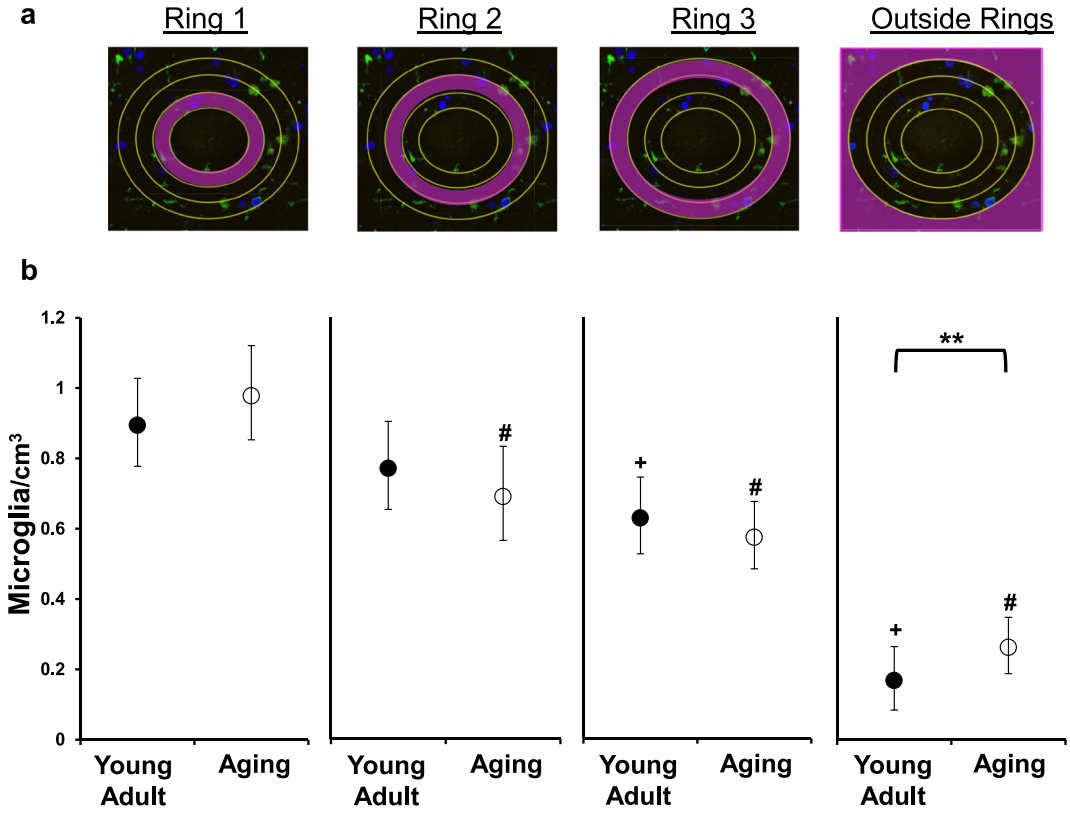

Fig. 2 Microglial density was greatest in close approximation to motor neurons in both young adult and aging dogs. **a** Using a modified Sholl's method (Sholl 1953), concentric rings were placed around each motor neuron cell body. Each ring increased in diameter by 6 μM, the average microglial cell body diameter (originally published in Toedebusch et al. 2018). The total numbers of microglia cells within each ring, and outside the ring system, were quantified. **b** A generalized linear mixed effect model with nested effects identified an interaction between ring and group. When the number of microglia within each ring for young adult dogs was compared, there was no difference between microglial number between ring 1 and ring 2 (223 observations; $p = 0.1723$), but ring 1 had increased microglia versus ring 3 ($p < 0.0001$) and versus outside the rings ($p < 0.0001$). In aging dogs, ring 1 had significantly increased number of microglia from all other rings and outside the rings (227 observations; $p < 0.0001$ all comparisons). Comparison of microglial number between young adult and aging dogs did not reveal differences in any of the rings (ring 1, $p = 0.5567$; ring 2, $p = 0.4763$; ring 3, $p = 0.5554$). However, the average number of microglia was increased in aging dogs compared with young adult dogs outside the ring system ($p = 0.0025$). Data is displayed as the estimated mean with 95% confidence interval. **, difference between young adult and aging dogs, $p < 0.01$; +, difference from ring 1 young adult dogs, $p < 0.001$; #, difference from ring 1 aging dogs, $p < 0.001$

adult dogs (74% vs. 18%; $p < 0.0001$). Of the activated microglia observed, young adult dogs had a higher proportion of anti-inflammatory microglia (76% vs. 24%; $p = 0.0009$), while aging dogs had an equivalent distribution between anti- and pro-inflammatory microglia (52% vs. 48%; $p = 0.36$).

To gain insight into the density of activated microglia cells around a particular motor neuron, we evaluated the number of arginase-1 or iNOS-expressing microglia per motor neuron. Therefore, in this analysis, we only considered motor neurons with nearby positively labeled microglia. We compared the average number of labeled microglia within and outside the ring system using a generalized linear model. Within the ring system, aging dogs had a decreased density of arginase-1-expressing microglia compared with young adult dogs (Fig. 5a; $p = 0.0027$). However, outside the ring system, this relationship was reversed, as aging dogs had an increased density of arginase-1-expressing microglia compared with young adult dogs (Fig. 5c; $p < 0.001$). Within the ring system, we observed no difference in the number of iNOS-expressing microglial between groups (Fig. 5b; $p = 0.3638$). However, iNOS-expressing microglial cell density was increased in aging dogs compared with young adult dogs outside of the ring system (Fig. 5d; $p < 0.001$). Additionally, there was an increased density of

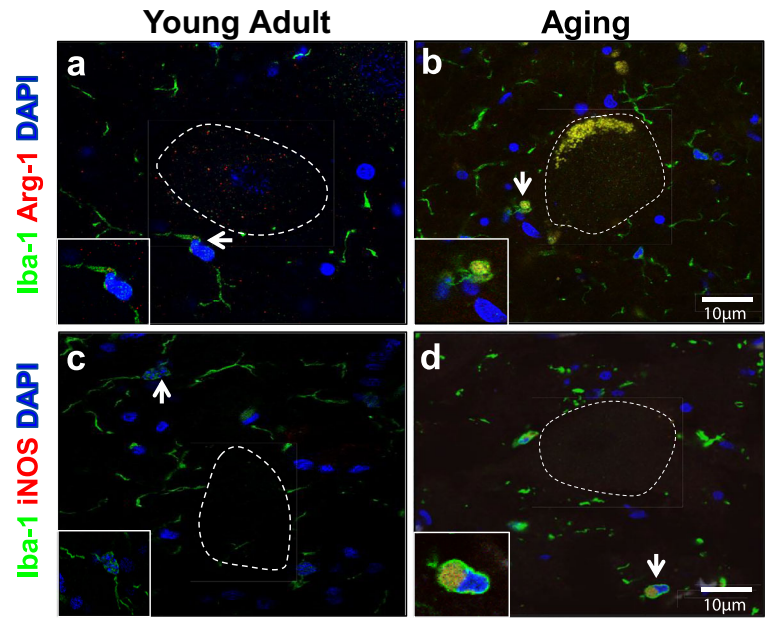

Fig. 3 Aging, but not young adult, microglia expressed both arginase-1 and inducible nitric oxide synthase (iNOS). Representative images of lumbar spinal cord microglia (Iba-1; green) in close proximity to motor neurons (outlined in white dotted line). **a** When observed, positive immunoreactivity for arginase-1 (Arg-1; orange) was punctate near the microglia nucleus in young adult dogs. **b** Diffuse arginase-1 immunoreactivity was commonly observed in the microglial cell body in aging dogs (originally published in Toedebusch et al. 2018). **c** The majority of young adult microglia did not demonstrate immunoreactivity for iNOS. **d** iNOS immunoreactivity localizes to the microglia cell body in aging dogs (originally published in Toedebusch et al. 2018). Scale bar 10 μM

arginase-1 and iNOS-expressing microglia within compared with outside the ring system in young adult dogs ($p < 0.001$; $p < 0.001$) and aging dogs ($p < 0.001$; $p < 0.001$).

Aging dog lumbar spinal cord, but not cervical spinal cord, has increased levels of mRNA for genes associated with reactive microglia compared with young adult dogs

Regional specificity in microglia phenotype has been previously demonstrated in dog spinal cord (Ensinger et al. 2010). To gain insights into the phenotypic state of microglia in aging dog spinal cord, we examined the levels of genes associated with pro-inflammatory versus anti-inflammatory phenotypes (Lively and Schlichter 2018) in young adult and aging dogs. Moreover, we evaluated a subset of genes encoding proteins involved in phagocytosis and proteolysis (Donkin et al. 2010; Jiang et al. 2008), which have been observed to have increased mRNA steady-state levels in microglia from neurodegenerative disease models (Chiu et al. 2013; Nikodemova et al. 2014).

In the cervical spinal cord, we observed no differences in steady-state levels between young adult and aging dogs for all genes examined (Fig. 6). However, in lumbar spinal cord, aging dogs had increased levels of both pro-inflammatory (*IL-6*; $p = 0.028$), and anti-inflammatory genes (*IL-1Rα*; $p = 0.005$) (Fig. 7) relative to young adult dogs. Moreover, aging dogs had significantly increased levels of phagocytic/proteolytic genes *ApoE* ($p = 0.047$), *C1QA* ($p = 0.029$), and *TREM2* ($p = 0.005$) (Fig. 7) relative to young adult dogs.

Discussion

Aging has a profound impact on the structure and function of the central nervous system (CNS). What is becoming increasingly clear is that these age-associated alterations might reflect changes in the aging CNS microenvironment. Microglia, a central constituent of the CNS microenvironment, continually monitor and respond to local environmental changes by altering their active state (Bickford et al. 2017). Not surprisingly, age-

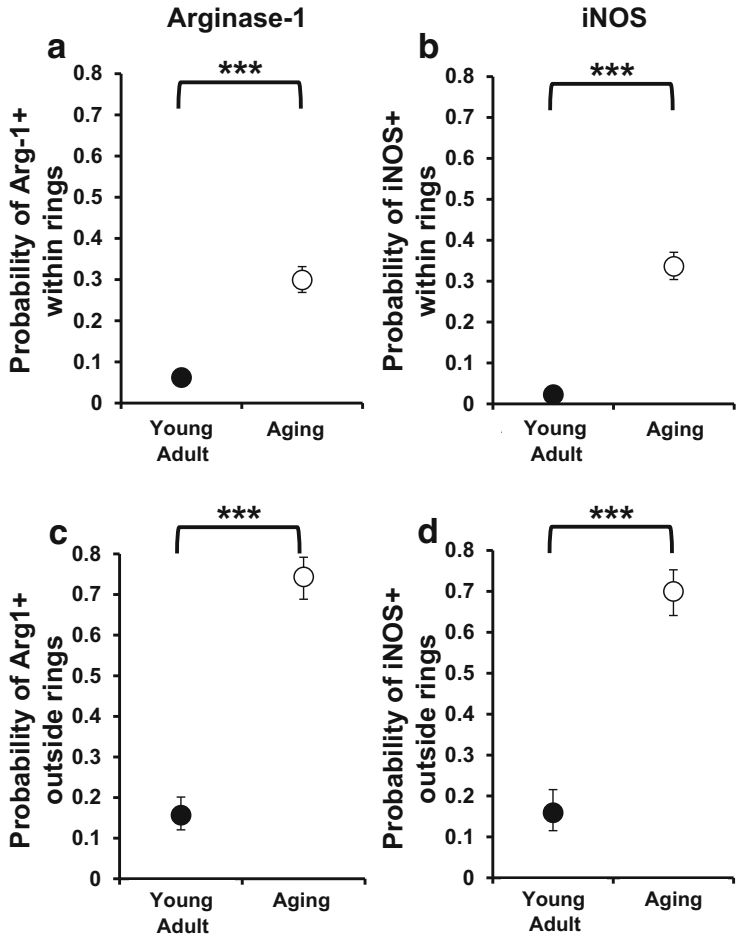

Fig. 4 The number of polarized microglia near motor neurons was increased in aging dogs. There was a greater probability of identifying microglia cells that expressed arginase-1 or iNOS close to motor neurons (**a**, **b**) or outside the ring system (**c**, **d**) in aging dogs relative to young adult dogs ($p < 0.001$ for all comparisons). Moreover, in both groups, this probability was higher outside the ring system (young adult dogs P = 0.0011; aging dogs p < 0.001). ***, difference between young adult and aging dogs, $p < 0.001$

related changes in microglia have been associated with molecular alterations in the aging CNS. Microglia in aged rat brains displayed hypertrophy of perinuclear cytoplasm and decreased process ramification (Conde and Streit 2006). Furthermore, aged microglia responded differently than young cells to local stimuli. Aged microglia responded more dramatically to pro-inflammatory signals while showing diminished, or even absent, responses to anti-inflammatory signals (Lee et al. 2013), referred to as age-related microglial priming (Bickford et al. 2017). Along with age-related molecular alterations, aging resulted in an increased susceptibility to neurodegenerative diseases such as Alzheimer's disease, Parkinson's disease, and amyotrophic lateral sclerosis (Niccoli and Partridge 2012). In fact, recent evidence correlates activated, phagocytic microglia with increasing cognitive decline in rhesus macaques (Shobin et al. 2017), underscoring the importance of microglia in the context of aging and age-related disease. However, what remains unclear is what role, if any, age-related alterations in CNS microenvironments contribute to disease susceptibility.

Age-related changes in CNS microenvironments are not necessarily uniform throughout the CNS. Regional differences in microglia have been observed in aging mouse brain (Grabert et al. 2016). Our analysis extended this observation to the spinal cord of aging dogs. mRNA levels demonstrated regional microglial differences in aging spinal cords. Based upon mRNA levels, lumbar microglia appeared more activated than microglia from cervical spinal cords (Figs. 6 and 7). Furthermore, our results suggested that the microenvironment near lumbar motor neurons was altered with aging. There was an increased number of motor neurons with nearby activated microglia in aging dogs (Table 2). As with our genetic analysis, the activation state of these microglia was not specifically polarized, as there were equal number of motor neurons with closely associated arginase-1 and iNOS-expressing

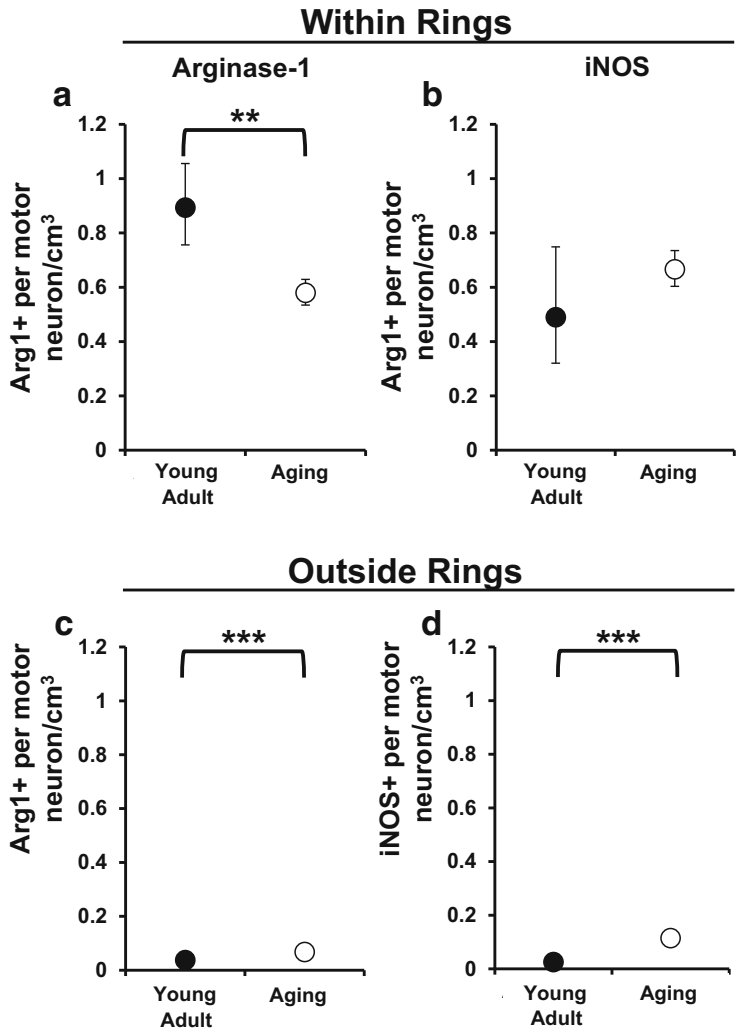

Fig. 5 Density of arginase-1-expressing microglial near motor neurons was decreased in aging dogs. We examined the number of arginase-1- (Arg-1+) or iNOS-expressing (iNOS+) microglia per motor neuron to determine the average density of each phenotype within (**a**, **b**) and outside (**c**, **d**) the ring system. **a** Compared with young adult dogs, Arg-1+ microglia per motor neuron was decreased in aging dogs (p = 0.0027). **b** There was no difference in the number of iNOS-expressing microglial cells per motor neuron between groups (p = 0.3638). **c** Outside the ring system, Arg-1+ (**c**) and iNOS+ (**d**) microglial cells were increased in aging dogs compared with young adult dogs (for both comparisons $p < 0.001$). **, difference between young adult and aging dogs, $p < 0.01$; ***, difference between young adult and aging dogs, $p < 0.001$

microglia (Table 2). Of note, aging dogs had both increased numbers of total microglia and an increase in the proportion of arginase-1 and iNOS-expressing microglia compared with young adult dogs, suggesting that the relative abundance of these two proteins was greater in aging dog spinal cord. However, we did not detect a difference in mRNA levels for these two genes. This may be due to differential production and/or turnover rates of these particular mRNAs and proteins. Furthermore, mRNA was quantified from spinal cord homogenate. Conversely, double-labeled microglial cells were counted, but the abundance of protein detected was not quantified. Therefore, while more cells expressed arginase-1 and iNOS in aging dogs, we cannot make conclusions regarding the relative protein abundance between groups.

Previous analyses suggested that the number of lumbar spinal cord microglia expressing markers associated with a pro-inflammatory phenotype was the same in aging and degenerative myelopathy (DM) affected dogs (Toedebusch et al. 2018). Both age and homozygosity of the mutant $SOD1^{E40K}$ allele were considered risk factors for developing DM (Awano et al. 2009; Zeng et al. 2014). However, while cells of the cervical spinal cord express only mutant $SOD1^{E40K}$, DM pathology invariantly began in the thoracolumbar spinal cord, resulting in reduced hindlimb motor function in affected dogs (Awano et al. 2009; Averill Jr 1973; March et al. 2009). Taken together with our current results, it is interesting to speculate that DM pathology initiates in the thoracolumbar spinal cord due to a confluence of risk factors, which suggests that

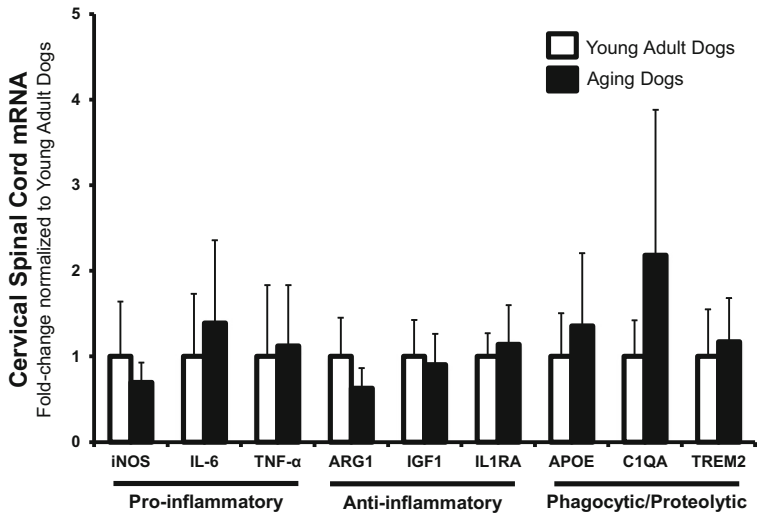

Fig. 6 Levels of microglia phenotypic markers were not different in the cervical spinal cord between young adult and aging dogs. mRNA levels of common pro-inflammatory (*iNOS*, *IL-6*, *TNF-α*), anti-inflammatory (*Arg-1*, *IGF-1*, *IL1Rα*), and phagocytic/proteolytic genes (*ApoE*, *C1QA*, *TREM2*) were not different between groups in hemisected C8 spinal cord segments. Data are displayed relative to young adult dogs. Young adult dogs, $n = 6$; aging dogs, $n = 5$. Comparisons based on unpaired t tests; bars represent group mean and standard error of the mean (SEM)

neither risk factor is sufficient to initiate DM on its own. We have demonstrated that microglia in aging cervical spinal cords are similar in phenotype to microglia in young adult cervical spinal cords. Thus, in aging cervical spinal cords, microglia are not yet primed. Therefore, the combination of primed microglia and mutant $SOD1^{E40K}$, as in the lumbar spinal cord, may be sufficient to trigger DM pathology.

Phagocytosis is an essential microglial function for maintenance of CNS homeostasis (Nadjar 2018). but there are regional differences in canine microglia phagocytic capacity (Ensinger et al. 2010). Importantly,

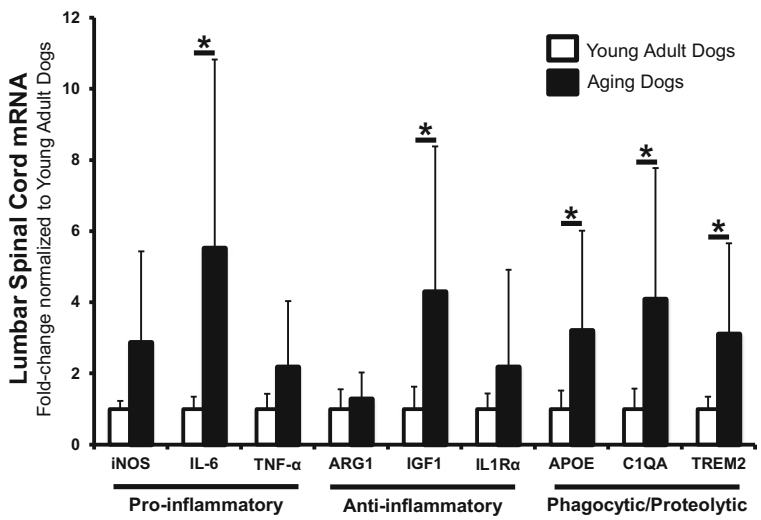

Fig. 7 Aging dog lumbar spinal cord had increased levels of genes associated with reactive microglia. mRNA levels of all pro-inflammatory markers were increased in aging dogs. However, only increases measured in IL-6 reached statistical significance. mRNA levels of anti-inflammatory markers IGF1 and IL1Rα were increased with IL1Rα increases reaching statistical significance. All phagocytic/proteolytic mRNA levels (*ApoE*, *C1QA*, *TREM2*) were significantly increased in L4 spinal cord segments in aging dogs. Data are displayed relative to young adult dogs. Young adult dogs, $n = 6$; aging dogs, $n = 5$. *$p < 0.05$. Comparisons based on unpaired t tests; bars represent group mean and standard error of the mean (SEM).

thoracolumbar spinal cord microglia had reduced phagocytic capacity compared with cervical spinal cord microglia (Ensinger et al. 2010). Furthermore, it has been well documented that aging results in reduced microglia phagocytic capacity (Floden and Combs 2011; Njie et al. 2012; Ritzel et al. 2015). While we did not directly evaluate microglia phagocytic function in this study, arginase-1 expression has been positively correlated with phagocytic activity (Cherry et al. 2015). In our study, there were more motor neurons with nearby arginase-1-expressing microglia in aging dogs, suggesting a regionally increased stimulus for microglial phagocytosis. However, while the density of total microglia near motor neurons was similar, the density of arginase-1 positive microglia was reduced in aging dogs relative to young adult dogs (Fig. 5). This may suggest that in the face of increased stimulus, the magnitude of the microglial phagocytic response was diminished in aging dogs. Thus, ineffective microglia phagocytosis may provide a sustained stimulus for pro-inflammatory microglial activation in the aging dog spinal cord.

Age-associated defects in blood-CNS barrier function, resulting in increased vascular permeability, have been documented in several species including mice (Hafezi-Moghadam et al. 2007), humans (Montagne et al. 2015), and dogs (Su et al. 1998). Notably, increased vascular permeability was increased in the aged spinal cord compared with the aged brain (Ritzel et al. 2015). Blood-spinal cord barrier (BSCB) compromise resulted in the accumulation of plasma proteins in the neuroparenchyma (Winkler et al. 2012) and has been recognized as a source of continued inflammation (Ritzel et al. 2015). Cerebrospinal fluid analysis in two aging dogs in this study demonstrated increased protein concentration with a normal cell count (data not shown), consistent with a compromised BSCB (Chen et al. 2012). Taken together, our data provokes the consideration that increased pro-inflammatory stimuli from a compromised BSCB, coupled with reduced microglia phagocytic capacity, might be sufficient to compromise the thoracolumbar microenvironment resulting in initial selective vulnerability for neurodegeneration.

Conclusions

We have demonstrated that regional functional specificity of canine spinal cord microglia is exacerbated with age. Increased insult to the spinal cord, coupled with phagocytic inefficiencies, may contribute to priming of lumbar, but not cervical, spinal cord microglia. Therefore, the stereotypic onset of DM pathology likely results from the culmination of several risk factors including the regional specificity of microglia priming, increasing age, and mutant $SOD1^{E40K}$. These findings warrant further study of aging canine microglia to further elucidate the complex mechanisms leading to microglia priming and the initiation of age-related neurodegenerative disease.

Funding information This work was supported by the American Kennel Club, Canine Health Foundation Clinician-Scientist Fellowship (C2902221).

Compliance with ethical standards All pet owners signed an informed consent form (approved by the University of Missouri Animal Care and Use Committee, protocol #8339). Young adult dogs (1 year of age) used in this study were research dogs housed at the University of Missouri in compliance with the National Institutes of Health Guide for the Care and Use of Laboratory Animals and approved by the University of Missouri Animal Care and Use Committee (protocol #8339).

References

Ahn JH, Choi JH, Kim JS, Lee HJ, Lee CH, Yoo KY, Hwang IK, Lee YL, Shin HC, Won MH (2011) Comparison of immunoreactivities in 4-HNE and superoxide dismutases in the cervical and the lumbar spinal cord between adult and aged dogs. Exp Gerontol 46:703–708

Averill DR Jr (1973) Degenerative myelopathy in the aging German Shepherd dog: clinical and pathologic findings. J Am Vet Med Assoc 15:1045–1051

Awano T, Johnson GS, Wade CM, Katz ML, Johnson GC, Taylor JF, Perloski M, Biagi T, Baranowska I, Long S, March PA, Olby NJ, Shelton GD, Khan S, O'Brien DP, Lindblad-Toh K, Coates JR (2009) Genome-wide association analysis reveals a SOD1 mutation in canine degenerative myelopathy that resembles amyotrophic lateral sclerosis. Proc Natl Acad Sci U S A 106:2794–2799

Beers DR, Henkel JS, Xiao Q, Zhao W, Wang J, Yen AA, Siklos L, McKercher S, Appel SH (2006) Wild-type microglia extend survival in PU.1 knockout mice with familial amyotrophic lateral sclerosis. Proc Natl Acad Sci U S A 103:16021–16026

Bickford PC et al (2017) Aging leads to altered microglial function that reduces brain resiliency increasing vulnerability to neurodegenerative diseases. Exp Gerontol 94:4–8

Boche D, Perry VH, Nicoll JA (2013) Review: Activation patterns of microglia and their identification in the human brain. Neuropathol Appl Neurobiol 39:3–18

Boillée S, Yamanaka K, Lobsiger CS, Copeland NG, Jenkins NA, Kassiotis G, Kollias G, Cleveland DW (2006) Onset and

progression in inherited ALS determined by motor neurons and microglia. Science. 312:1389–1392

Chen CP, Chen RL, Preston JE (2012) The influence of ageing in the cerebrospinal fluid concentrations of proteins that are derived from the choroid plexus, brain, and plasma. Exp Gerontol 47:323–328

Cherry JD et al (2015) Arginase 1+ microglia reduce Abeta plaque deposition during IL-1beta-dependent neuroinflammation. J Neuroinflammation 12:203

Chiu IM, Morimoto ET, Goodarzi H, Liao JT, O'Keeffe S, Phatnani HP, Muratet M, Carroll MC, Levy S, Tavazoie S, Myers RM, Maniatis T (2013) A neurodegeneration-specific gene-expression signature of acutely isolated microglia from an amyotrophic lateral sclerosis mouse model. Cell Rep 4: 385–401

Chung JY et al (2010) Comparison of ionized calcium-binding adapter molecule 1-immunoreactive microglia in the spinal cord between young adult and aged dogs. Neurochem Res 35:620–627

Coates JR, Wininger FA (2010) Canine degenerative myelopathy. Vet Clin North Am Small Anim Pract 40:929–950

Colton CA (2009) Heterogeneity of microglial activation in the innate immune response in the brain. J NeuroImmune Pharmacol 4:399–418

Conde JR, Streit WJ (2006) Microglia in the aging brain. J Neuropathol Exp Neurol 65:199–203

Crain JM, Nikodemova M, Watters JJ (2013) Microglia express distinct M1 and M2 phenotypic markers in the postnatal and adult central nervous system in male and female mice. J Neurosci Res 91:1143–1151

Donkin JJ, Stukas S, Hirsch-Reinshagen V, Namjoshi D, Wilkinson A, May S, Chan J, Fan J, Collins J, Wellington CL (2010) ATP-binding cassette transporter A1 mediates the beneficial effects of the liver X receptor agonist GW3965 on object recognition memory and amyloid burden in amyloid precursor protein/presenilin 1 mice. J Biol Chem 285:34144–34154

Ensinger E-M, Boekhoff TM, Carlson R, Beineke A, Rohn K, Tipold A, Stein VM (2010) Regional topographical differences of canine microglial immunophenotype and function in the healthy spinal cord. J Neuroimmunol 227:144–152

Floden AM, Combs CK (2011) Microglia demonstrate age-dependent interaction with amyloid-beta fibrils. J Alzheimers Dis 25:279–293

Frank MG, Barrientos RM, Biedenkapp JC, Rudy JW, Watkins LR, Maier SF (2006) mRNA up-regulation of MHC II and pivotal pro-inflammatory genes in normal brain aging. Neurobiol Aging 27:717–722

Godbout JP, Chen J, Abraham J, Richwine AF, Berg BM, Kelley KW, Johnson RW (2005) Exaggerated neuroinflammation and sickness behavior in aged mice following activation of the peripheral innate immune system. FASEB J 19:1329–1331

Grabert K, Michoel T, Karavolos MH, Clohisey S, Baillie JK, Stevens MP, Freeman TC, Summers KM, McColl B (2016) Microglial brain region-dependent diversity and selective regional sensitivities to aging. Nat Neurosci 19:504–516

Graeber MB (2010) Changing face of microglia. Science. 330: 783–788

Hafezi-Moghadam A, Thomas KL, Wagner DD (2007) ApoE deficiency leads to a progressive age-dependent blood-brain barrier leakage. Am J Phys Cell Phys 292:C1256–C1262

Hefendehl JK, Neher JJ, Sühs RB, Kohsaka S, Skodras A, Jucker M (2014) Homeostatic and injury-induced microglia behavior in the aging brain. Aging Cell 13:60–69

Isobe K, Cheng Z, Nishio N, Suganya T, Tanaka Y, Ito S (2014) iPSCs, aging and age-related diseases. New Biotechnol 31: 411–421

Jiang Q, Lee CY, Mandrekar S, Wilkinson B, Cramer P, Zelcer N, Mann K, Lamb B, Willson TM, Collins JL, Richardson JC, Smith JD, Comery TA, Riddell D, Holtzman DM, Tontonoz P, Landreth GE (2008) ApoE promotes the proteolytic degradation of Abeta. Neuron. 58:681–693

Krabbe G et al (2013) Functional impairment of microglia coincides with beta-amyloid deposition in mice with Alzheimer-like pathology. PLoS One 8:e60921

Lee DC, Ruiz CR, Lebson L, Selenica ML, Rizer J, Hunt JB Jr, Rojiani R, Reid P, Kammath S, Nash K, Dickey CA, Gordon M, Morgan D (2013) Aging enhances classical activation but mitigates alternative activation in the central nervous system. Neurobiol Aging 34:1610–1620

Lewis KE et al (2014) Microglia and motor neurons during disease progression in the SOD1G93A mouse model of amyotrophic lateral sclerosis: changes in arginase1 and inducible nitric oxide synthase. J Neuroinflammation 11:55

Liao B, Zhao W, Beers DR, Henkel JS, Appel SH (2012) Transformation from a neuroprotective to a neurotoxic microglial phenotype in a mouse model of ALS. Exp Neurol 237:147–152

Livak K, 1997. Comparative Ct method. ABI Prism 7700 Sequence Detection System. User Bulletin no. 2 PE Applied Biosystems, CA, USA.

Lively S, Schlichter LC (2018) Microglia responses to pro-inflammatory stimuli (LPS, IFNgamma+TNFalpha) and reprogramming by resolving cytokines (IL-4, IL-10). Front Cell Neurosci 12:215

March PA, Coates JR, Abyad RJ, Williams DA, O'Brien DP, Olby NJ, Keating JH, Oglesbee M (2009) Degenerative myelopathy in 18 Pembroke Welsh Corgi dogs. Vet Pathol 46:241–250

Montagne A, Barnes SR, Sweeney MD, Halliday MR, Sagare AP, Zhao Z, Toga AW, Jacobs RE, Liu CY, Amezcua L, Harrington MG, Chui HC, Law M, Zlokovic BV (2015) Blood-brain barrier breakdown in the aging human hippocampus. Neuron. 85:296–302

Morris SM Jr (2004) Enzymes of arginine metabolism. J Nutr 134: 2743S–2747S discussion 2765S-2767S

Nadjar A (2018) Role of metabolic programming in the modulation of microglia phagocytosis by lipids. Prostaglandins Leukot Essent Fat Acids 135:63–73

Niccoli T, Partridge L (2012) Ageing as a risk factor for disease. Curr Biol 22:R741–R752

Nikodemova M, Small AL, Smith SM, Mitchell GS, Watters JJ (2014) Spinal but not cortical microglia acquire an atypical phenotype with high VEGF, galectin-3 and osteopontin, and blunted inflammatory responses in ALS rats. Neurobiol Dis 69:43–53

Nimmerjahn A, Kirchhoff F, Helmchen F (2005) Resting microglial cells are highly dynamic surveillants of brain parenchyma in vivo. Science. 308:1314–1318

Njie EG et al (2012) Ex vivo cultures of microglia from young and aged rodent brain reveal age-related changes in microglial function. Neurobiol Aging 33:195.e1–195.12

Reu P et al (2017) The lifespan and turnover of microglia in the human brain. Cell Rep 20:779–784

Ritzel RM, Patel AR, Pan S, Crapser J, Hammond M, Jellison E, McCullough L (2015) Age- and location-related changes in microglial function. Neurobiol Aging 36:2153–2163

Schafer DP, Lehrman EK, Kautzman AG, Koyama R, Mardinly AR, Yamasaki R, Ransohoff RM, Greenberg ME, Barres BA, Stevens B (2012) Microglia sculpt postnatal neural circuits in an activity and complement-dependent manner. Neuron. 74:691–705

Sheffield LG, Berman NE (1998) Microglial expression of MHC class II increases in normal aging of nonhuman primates. Neurobiol Aging 19:47–55

Shobin E, Bowley MP, Estrada LI, Heyworth NC, Orczykowski ME, Eldridge SA, Calderazzo SM, Mortazavi F, Moore TL, Rosene DL (2017) Microglia activation and phagocytosis: relationship with aging and cognitive impairment in the rhesus monkey. Geroscience. 39:199–220

Sholl DA (1953) Dendritic organization in the neurons of the visual and motor cortices of the cat. J Anat 87:387–406

Su MY, Head E, Brooks WM, Wang Z, Muggenburg BA, Adam GE, Sutherland R, Cotman CW, Nalcioglu O (1998) Magnetic resonance imaging of anatomic and vascular characteristics in a canine model of human aging. Neurobiol Aging 19:479–485

Svahn AJ, Becker TS, Graeber MB (2014) Emergent properties of microglia. Brain Pathol 24:665–670

Toedebusch CM, Snyder JC, Jones MR, Garcia VB, Johnson GC, Villalón EL, Coates JR, Garcia ML (2018) Arginase-1 expressing microglia in close proximity to motor neurons were increased early in disease progression in canine degenerative myelopathy, a model of amyotrophic lateral sclerosis. Mol Cell Neurosci 88:148–157

Tremblay ME et al (2010) Microglial interactions with synapses are modulated by visual experience. PLoS Biol 8:e1000527

Tremblay ME, Stevens B, Sierra A, Wake H, Bessis A, Nimmerjahn A (2011) The role of microglia in the healthy brain. J Neurosci 31:16064–16069

Untergasser A et al (2012) Primer3–new capabilities and interfaces. Nucleic Acids Res 40:e115

Urfer SR, Kaeberlein TL, Mailheau S, Bergman PJ, Creevy KE, Promislow DE, Kaeberlein M (2017a) Asymptomatic heart valve dysfunction in healthy middle-aged companion dogs and its implications for cardiac aging. Geroscience. 39:43–50

Urfer SR, Kaeberlein TL, Mailheau S, Bergman PJ, Creevy KE, Promislow DEL, Kaeberlein M (2017b) A randomized controlled trial to establish effects of short-term rapamycin treatment in 24 middle-aged companion dogs. Geroscience. 39: 117–127

Varnum MM, Ikezu T (2012) The classification of microglial activation phenotypes on neurodegeneration and regeneration in Alzheimer's disease brain. Arch Immunol Ther Exp 60:251–266

Winkler EA, Sengillo JD, Bell RD, Wang J, Zlokovic BV (2012) Blood-spinal cord barrier pericyte reductions contribute to increased capillary permeability. J Cereb Blood Flow Metab 32:1841–1852

Xie Z, Morgan TE, Rozovsky I, Finch CE (2003) Aging and glial responses to lipopolysaccharide in vitro: greater induction of IL-1 and IL-6, but smaller induction of neurotoxicity. Exp Neurol 182:135–141

Zeng R, Coates JR, Johnson GC, Hansen L, Awano T, Kolicheski A, Ivansson E, Perloski M, Lindblad-Toh K, O'Brien DP, Guo J, Katz ML, Johnson GS (2014) Breed distribution of SOD1 alleles previously associated with canine degenerative myelopathy. J Vet Intern Med 28:515–521